and $F^-$ are about 60 and 30%, respectively. These estimates are consistent with the changes observed in both the ESR and $^{19}F$ NMR experiments.

The model proposed here—one equatorial and one axial binding site for exogenous ligands—is compatible with the known five-coordinate chemistry of copper(II) centers.[34] If it is assumed that the GOase Cu(II) site consists of three equatorially coordinated endogenous ligands from the protein matrix, one labile equatorially coordinated ligand (in the native enzyme, $H_2O$ or, possibly, $OH^-$) and a quite labile, weakly bound axially coordinated ligand (again in the native enzyme, $H_2O$), a square-pyramidal five-coordinate geometry would be present. In such Cu(II) complexes the axial bond distances are always significantly longer than equatorial ones. Thus ligands which would bind potentially via $\pi$ bonds would coordinate preferentially at an equatorial site and would tend to stabilize four coordinate compared to five-coordinate geometries. This latter dictum can be interpreted in terms of competition for the same Cu(II) orbitals required for $\pi$ bonds by both axial and equatorial ligands. Thus poor $\pi$-bonding ligands (e.g., $F^-$, $H_2O$) do not compete effectively with $CN^-$ for an equatorial binding site. On the other hand, if $CN^-$ is already equatorially coordinated, a second $CN^-$ would be less likely to coordinate axially; in the case at hand, $F^-$ (a "hard" ligand that binds predominantly through $\sigma$ bonds) would compete effectively against excess $CN^-$ for an axial site. The result that axially coordinated $F^-$ binds more weakly than does equatorially coordinated $F^-$ can be rationalized in terms of the longer bond distance for the former, a general feature of Cu(II) square-pyramidal five-coordinate geometry. The same argument can be used to justify the inference that axially coordinated $F^-$ exchanges relatively rapidly with bulk $F^-$ compared to equatorially coordinated $F^-$. Thus, for a five-coordinate Cu(II) square-pyramidal complex in which one fluoride was coordinated at an equatorial site and one at an axial position, one would expect $CN^-$ to displace preferentially the equatorial $F^-$ and also to find that the bonding of the axial $F^-$ is weaker in the $CN^-$ complex. Such effects are just those which have been inferred from the $^{19}F$ NMR relaxation measurements.

In summary, we conclude that the presence of two Cu(II) coordination sites in GOase for exogenous ligands is established by these results. The data presented in support of a high affinity, equatorial ligand site augment ESR results reported previously.[5b,c,11] That anions (and water) bind also, albeit weakly, to an axial site is a suggestion that may be relevant to the coordination of hydroxyl groups of substrate ligands.[5a] Moreover, the electronic interaction between Cu(II) and axially coordinated ligand can be modified, as shown in this work, if the labile equatorial ligand ($H_2O$ or $OH^-$) ordinarily present is replaced by a strong $\pi$-bonding ligand such as $CN^-$. Thus this modulation may be related to the properties of these exogenous ligands as noncompetitive inhibitors[27] (i.e., inhibitors which do not seriously effect GOase substrate binding but do block enzyme catalysis). Kinetic and magnetic resonance studies are being carried out to elucidate the relationship between the bonding properties of an equatorially coordinated exogenous ligand and its effect on catalysis.

**Acknowledgment.** B.J.M. gratefully acknowledges fellowships from the Allied Chemical Corp. and from the Graduate School, SUNY/Buffalo. We thank the National Science Foundation for support for this research (Grant No. BMS73-01248-A01) and for some of the NMR instrumentation used (Grant No. CHE7506183-A02 to the Department of Chemistry, SUNY/Buffalo). We also thank our colleagues in the Bioinorganic Graduate Research Group for stimulating and helpful discussions.

(34) B. J. Hathaway and D. E. Billing, *Coord. Chem. Rev.*, **5**, 143 (1970), and references therein.

# Electron Paramagnetic Resonance Study of Nitrosylhemoglobin and Its Chemistry in Single Crystals

**D. C. Doetschman* and S. G. Utterback**[1]

*Contribution from the Department of Chemistry, State University of New York at Binghamton, Binghamton, New York.* *Received July 21, 1980*

**Abstract:** The electron paramagnetic resonance (EPR) of nitrosylhemoglobin (HbNO) is measured in single crystals of converted human oxyhemoglobin ($HbO_2$). Several chemical and physical processes in the crystals are observable by means of the EPR. At 9 °C $HbO_2$ a subunits exchange $O_2$ for NO faster than b subunits. The subunit spectra display both $^{14}NO$ and [$^{14}N$]histidine hyperfine structure. Power saturation between 1.6 and 4.2 K and temperature dependence above 80 K point to efficient spin–spin and spin–lattice relaxation processes that involve heme–heme magnetic dipolar interactions between both kinds of subunits. With a Hg–Xe lamp, HbNO photolysis quickly occurs at 4.2 K, resulting in the disappearance of the EPR spectrum. The HbNO spectrum returns when the sample is warmed from 4.2 to 85 K.

Nitrosylhemoglobin (HbNO) resembles the physiologically important oxyhemoglobin ($HbO_2$) in several ways, presumably because of similar electronic structures.[2-5] Moreover, HbNO has the advantage of spin $S = {}^1/_2$ in the highest occupied molecular orbital, making electron paramagnetic resonance (EPR) possible, as first shown by Gordy and Rexrod.[6] The heme structures in HbNO and a free model oxyheme are very similar:[7-8] the FeNO and FeOO bond angles are less than 180° and in both structures more than one type of diatomic molecule projection on the heme

(1) From dissertation research in partial fulfillment of Ph.D. requirements.
(2) Kon, H. *J. Biol. Chem.* **1968**, *243*, 4350.
(3) Kon, H. *Biochemistry* **1969**, *8*, 4757.
(4) Doetschman, D. C. *Chem. Phys.* **1980**, *48*, 307.
(5) Doetschman, D. C.; Schwartz, S. A.; Utterback, S. G. *Chem. Phys.* **1980**, *49*, 1.
(6) Gordy, W.; Rexrod, H. N. In "Free Radicals in Biological Systems", Blois, M. S., Ed., Academic Press: New York; 1961.
(7) Deatherage, J. F.; Moffat, K. *J. Mol. Biol.* **1979**, *134*, 401.
(8) Collman, J. P.; Gagney, R. R.; Reed, C. A.; Halberty, T. R.; Lang, G.; Robinson, W. T. *J. Am. Chem. Soc.* **1975**, *97*, 1427.

0002-7863/81/1503-2847$01.25/0 

plane is found. Some circumstantial evidence from HbNO EPR even exists for a phosphate-mediated cooperative Bohr effect in solution.[9-11]

The process of NO uptake and release in HbNO are particularly relevant because the corresponding $O_2$ processes in $HbO_2$ are the ultimate focus of all hemoglobin work. EPR studies in single crystals resolve the individual heme subunits in the intact tetramer, as has been demonstrated in horse HbNO crystals.[11] To be able to monitor the uptake and release of the diatomic ligand with the resolution of each heme subunit would be ideal. One could also examine the subunit spectra closely for evidence of cooperativity, i.e., interactions between heme subunits. This study is a report of our attempt to see if these phenomena could be monitored by EPR spectroscopy in single crystals containing HbNO.

Human, rather than horse,[11] $HbNO/O_2$ crystals are chosen because of their high tetragonal space group symmetry $P4_12_12$ with $Z = 4$.[12] Monoclinic horse HbNO has a simple spectrum but low symmetry.[11] High-crystal symmetry can be used to tremendous advantage in the EPR experiment and the spectrum analysis, in spite of spectral congestion.[13] For example, when the field is parallel to the tetragonal axis, all $\alpha$ subunit spectra become identical and all $\beta$ likewise. Therefore, this particular field orientation makes the easy resolution of $\alpha$ and $\beta$ spectra possible too.

The $HbO_2$ crystals are grown first by Drabkin and Perutz'[14] method and then some of the $O_2$ ligand is exchanged for NO chemically generated in the mother liquor. The method itself incidentally provides an opportunity to observe different rates of exchange on the $\alpha$ and $\beta$ subunits by means of the crystal EPR spectra.

The traditional method of studying diatomic molecule ligand uptake and release, however, is the photochemical method developed by Gibson,[15a] whose kinetic studies reveal different ligand binding rates in the $\alpha$ and $\beta$ chains.[15b-f] While the HbNO photodissociation quantum yield of NO and five-coordinate heme is 0.001 in solution near room temperature,[16] appreciable photolysis occurs at lower temperatures. Mössbauer[17] and EPR[18] studies of frozen HbNO solutions at 4.2 K show that nearly complete photolysis can be accomplished in a few minutes time with ~ 100-W tungsten lamps. The studies also show that complete recombination takes place when the samples are warmed to 77 K. Optical measurements of CO recombination after photolysis at low temperatures on frozen solutions of CO-protoheme,[19] CO-myoglobin,[20,21] and CO-hemoglobin (HbCO)[22] have been very fruitful. Several CO rebinding steps, one of which may occur by tunneling, are identified along with the associated energy barriers. Therefore we choose to monitor NO uptake and relase with EPR by photolyzing the HbNO in single crystals at 4.2 K and by subsequently raising the temperature of the crystal.

## Experimental Section

**Hemoglobin Separation.**[23] Human erythrocytes are concentrated by centrifugation and washed with 0.9% NaCl. The solids from another centrifugation (10 min, 10000 rpm, 4 °C) are lysed with an equal volume of distilled $H_2O$ and the cell debris centrifuged down for disposal (1 h, 14000 rpm, 4 °C). The supernatant is dialyzed and chromatographed (pH 8.5 Tris buffered DE 52 column) to separate adult hemoglobin from the fetal form and other proteins.

**Oxyhemoglobin Crystal Growth.**[14] To an inorganic buffered (1.6 M phosphate, pH 6.7) hemoglobin solution (4% by weight) is added 4 M inorganic buffer, forming a narrow range of approximately saturated 1% solutions in crystal growing vials. The vials are sealed and refrigerated at 9 °C after the traditional drop of toluene was added. Bipyramidal $HbO_2$ crystals (0.5–1.0 mm) salt out in 2–3 weeks. The crystals keep up to 4 weeks before appreciable degradation (according to visible absorption[24] and HbNO EPR line broadening) in the HbNO form.

**Conversion to Nitrosylhemoglobin.** Well-formed crystals, selected under a microscope, are pipetted with a drop of mother liquor to an isoionic nitrite/ascorbate solution (0.005 M $NaNO_2$, 1.0 M sodium ascorbate, pH 6.7 inorganic phosphate buffer). The method previously applied to solutions[25,26] results in gradual conversion of the crystals over several days (according to solution EPR[2,3] and optical absorption spectra[24] of dissolved crystals).

**HbNO Crystal EPR.** An HbNO crystal in a droplet of mother liquor is pipetted into a silica EPR sample tube and oriented under a microscope, and the droplet is removed with a rolled tissue. One end of the cylindrical sample tube is friction fitted with Teflon tape into a brass collet on whose periphery gear teeth are machined. The part of the sample tube beyond the collet gear is inserted horizontally into a TE 102 EPR cavity. The sample, cavity, and attached copper-constantan thermocouple junction are inserted into the cryostat (modified Janis 6 RD) tail.

During the experiment the sample is oriented with a vertical rod ending in a worm which rotates the collet gear and sample tube. The cryostat tail is situated between the poles of an electromagnet (Varian, 9 in) which can be rotated around the vertical tail. The horizontal crystal and vertical magnet rotation axes permit any desired field orientation in the sample. A computer program is used to calculate crystal and field dial settings for serial rotations in three mutually perpendicular planes from any two crystal symmetry axes measured in an experiment. The EPR specra are measured with a Varian V-4500 X-band EPR spectrometer which employs phase-sensitive detection at the 100-kHz field-modulation frequency. The modulation is applied through coils mounted on the sides of the cavity.

The sample and cavity insert are cooled by filling the outer reservoir of the cryostat with $N_2(l)$. The inner reservoir is cooled to the range 80–273 K by means of $N_2(l)$ below the cavity and with a variable flow of cold $N_2(g)$ from a $N_2(l)$ heat exchanger. The temperature is determined with the thermocouple against crushed ice slush standard. At 4.2 K the inner reservoir is filled with He(l) at 1 atm, immersing the sample. Temperatures between 1.2 and 4.2 K are reached by pumping the reservoir with two Stokes pumps of 80- and 30-cfm capacities to reduced He pressures which are measured with a McLoed gauge to determine the temperature. Temperatures between 4.2 and 80 K are traversed without control after the liquid helium vaporizes. The thermocouple is capable of temperature measurement (±3 K) above 50 K.

**Photolysis.** The silica sample tube, the grid bottom on the cavity, and the set of silica windows on the bottom of the cryostat permit irradiation of the sample from below. Light from a 1000-W Oriel Hg–Xe lamp arc is collimated with a 5-cm $f/1$ silica lens, directed through an iris and shutter, reflected with a mirror to another silica lens focused ($f = 10$ cm) on the crystal. Alternatively 6.5-mJ 337-nm $N_2$ laser pulses from a

(9) (a) Trittlevitz, E.; Sick, H.; Gersonde, K. *Eur. J. Biochem.* **1972**, *31*, 578. (b) Rein, H.; Ristan, D.; Scheler, W. *FEBS Lett.* **1972**, *24*, 24. (c) Trittlevitz, E.; Gersonde, K.; Winterhalter, K. H. *Eur. J. Biochem.* **1975**, *51*, 33. (d) Shiga, T.; Hwang, K. J.; Tyuma, I. *Biochemistry* **1969**, *8*, 378.
(10) (a) Perutz, M. F. *Nature (London)* **1970**, *228*, 726; **1970**, *228*, 726. (b) *Ibid.* 734.
(11) Chien, J. C. W. *J. Chem. Phys.* **1969**, *51*, 4220.
(12) Perutz, M. F.; Liquori, A. M.; Eirich, F. *Nature (London)* **1951**, *167*, 929.
(13) Doetschman, D. C.; McCool, B. J. *Chem. Phys.* **1975**, *8*, 1.
(14) (a) Drabkin, D. L. *J. Biol. Chem.* **1946**, *164*, 703. (b) Perutz, M. F. *J. Cryst. Growth* **1968**, *2*, 54.
(15) (b) Gibson, Q. H. *J. Physiol.* **1956**, *134*, 112, 123; (b) *J. Biol. Chem.* **1970**, *245*, 3285; (c) *Proc. Nat. Acad. Sci. USA* **1973**, *70*, 1. (d) Gibson, Q. H.; Nagel, R. L. *J. Biol. Chem.* **1977**, *249*, 7255. (e) Olson, J. S.; Gibson, Q. H. *Ibid.* **1971**, *246*, 5241. (f) Olson, J. S.; Andersen, M. E.; Gibson, Q. H. *Ibid.* **1971**, *246*, 5919.
(16) Ainsworth, S.; Gibson, Q. H. *Nature (London)* **1957**, *180*, 1416.
(17) Spartalian, K.; Lang, G.; Yonetani, T. *Biochim. Biophys. Acta* **1976**, *428*, 281.
(18) Nagai, K.; Hori, H.; Yoshida, S.; Sakamoto, H.; Morimoto, H. *Biochim. Biophys. Acta* **1978**, *532*, 17.
(19) Alberding, N.; Austin, R. H.; Beeson, K. W.; Chan, S. S.; Eisenstein, L.; Frauenfelder, H. M.; Nordland, T. M. *Science (Washington, DC)* **1976**, *192*, 1002.
(20) Austin, R. H.; Beeson, K. W.; Eisenstein, L.; Frauenfelder, H.; Gunsalus, I. C.; Marshall, V. P. *Phys. Rev. Lett.* **1974**, *32*, 403.
(21) Austin, R. H., Beeson, K. W., Eisenstein, L.; Frauenfelder, H.; Gunsalus, I. C. *Biochemistry* **1975**, *14*, 5355.
(22) Alberding, N.; Austin, R. H., Chan. S. S. Eisenstein, L.; Frauenfelder, H.; Gunsalus, I. C.; Nordland, T. M. *J. Chem. Phys.* **1976**, *65*, 4701.
(23) (a) Benesch, R. E.; Benesch, R. *Biochemistry* **1962**, *1*, 735. (b) Geraci, G.; Parkhust, L.; Gibson, Q. H. *J. Biol. Chem.* **1969**, *244*, 4664. DeYoung, A.; Pennelly, R. R.; Tan-Wilson, A. L.; Noble, R. W. *Ibid.* **1976**, *251*, 6692.
(24) Antonini, E.; Brunori, M. "Hemoglobin and Myoglobin in their Reactions with Ligands", in Frontiers of Biology, ed. by Neuberger, A., and Tatum, E. L., North-Holland Publishing Co.: Amsterdam, 1971.
(25) (a) Coryell, C. D. Pauling, L.; Dodson, R. W., *J. Phys. Chem.* **1939**, *43*, 825. (b) Yonetani, T.; Yamamoto, H.; Erman, J. E.; Leigh, J. S., Jr.; Reed, G. H., *J. Biol. Chem.* **1972**, *247*, 2447.
(26) Trittelvitz, E.; Gersonde, K.; Winterhalter, K. H. *Eur. J. Biochem.* **1975**, *51*, 33.

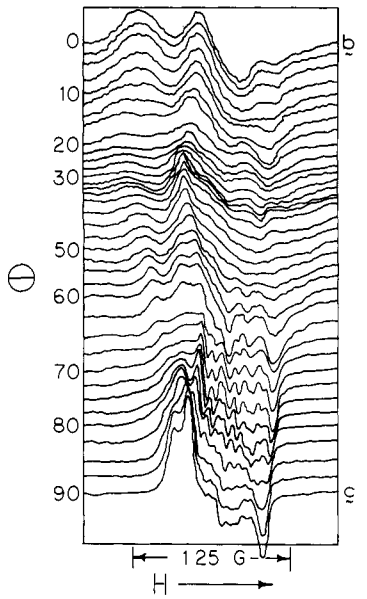


**Figure 1.** X-band EPR spectrum of a single crystal of human nitrosylhemoglobin at 80 K with the magnetic field in the *bc* plane taken in 2.5° intervals. The field at the center of the 250-G sweep is 3240 G, and the microwave frequency is 9.1930 GHz.

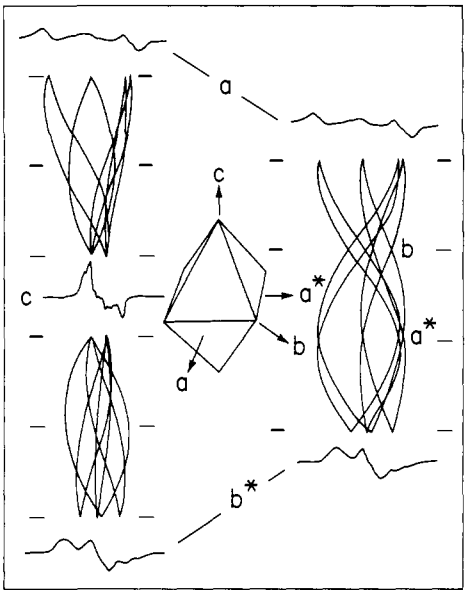


**Figure 2.** Angular dependence of the EPR spectra of the subunits in the principal crystal planes of HbNO. Shown are the principal crystal axis spectra and a sketch of the typical crystal morphology. The curves shown are preliminary fits to experimental points in the serial rotations. The spectra are under the conditions of Figure 1.

Lumonics K-261-2 excimer laser were similarly directed to the mirror and thence to the crystal.

## Results and Discussion

**(I) HbNO Crystal EPR.** The HbNO spectra are measured at 2.5° intervals in serial rotations in the three principal crystal planes, *ab*, *ac*, and *bc*. The crystals are typically octahedra slightly elongated between two apexes along the four fold *c* axis. The four equivalent corners are bisected by the twofold (heme dyad) axes, which we call the *b* axes. The edges between these corners are parallel to the twofold screw *a* axes and 45° from the *b* axes. A typical serial rotation is shown in Figure 1 for the *bc* plane.

On the basis of the $HbO_2$ space group symmetry, a single $\alpha$ subunit spectrum and a single $\beta$ subunit spectrum is predicted for HbNO when the field $H\|c$. Likewise two different $\alpha$ and two different $\beta$ spectra appear when $H\|a,b$. Otherwise there are four different spectra for each subunit with the field in a principal

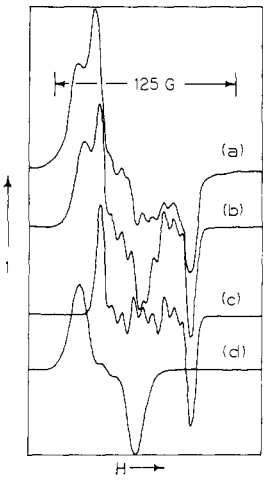


**Figure 3.** EPR spectrum of HbNO crystal with $H\|c$ and its simulated spectrum: (a) experimental spectrum taken under the conditions of Figure 4; (b) spectrum simulated by adding the a- and b-subunit spectra; (c) b subunit spectrum; (d) a subunit spectrum. See text for line-shape parameters.

Table I. Preliminary Principal *g* Values of the Subunits in Human Nitrosylhemoglobin Single Crystals at 85 K[a]

| subunit | $g_x$ | $g_y$ | $g_z$ |
|---|---|---|---|
| a | 2.0548 (0.0035) | 1.9723 (0.0055) | 2.0054 (0.0018) |
| b | 2.0697 (0.0005) | 1.9855 (0.0015) | 2.0071 (0.0009) |

[a] Standard deviations are in parentheses.

crystal plane. The spectra along these field directions interconnect with one another in the serial rotations as shown in Figure 2.

The spectrum with $H\|c$ can be simulated with a sum of $\alpha$ and $\beta$ subunit spectra with characteristic $^{14}N$ hyperfine patterns together with a weak unidentified single peak. The simulation and the two separate subunit spectra are compared with the measured spectrum in Figure 3. In this direction the narrow-line upfield subunit displays both a $^{14}NO$ hyperfine pattern and presumably a [$^{14}N$]histidine hyperfine pattern while the broad-line downfield spectrum displays only the $^{14}NO$ hyperfine pattern. While the former is probably the $\beta$ subunit and the latter the $\alpha$, the asignment is tentative and the subunits will be called b subunits and a subunits. The b simulation is with $g = 2.014$, a($^{14}NO$) = 54 MHz, $a$([$^{14}N$]histidine) = 18 MHz, with line widths of 9 MHz between 1/e points. The a has $g = 2.024$, a ($^{14}NO$) = 36 and 19 MHz widths. The remaining disagreement belongs to the unidentified line.

The observation (see II) that NO uptake by $HbO_2$ crystals is faster for a subunits than for b subunits makes it possible to prepare predominantly a-HbNO which facilitates the identification of a-subunit lines in the spectrum. In Figure 2 are shown the two a- and the two b-subunit spectra that appear when $H\|a$ and when $H\|b$, consistent with space group symmetry. An a and b line partially overlap at the low $g$ end of the $H\|a$ spectrum and in the middle of the $H\|b$ spectrum. On the basis[27] of the parametric dependence on $2\theta$ of the interconnecting curves, the preliminary principal $g$ values given in Table I are obtained. The 54-MHz and 35-MHz $^{14}NO$ hyperfine splittings observed with $H\|c$ are comparable with the value of 55 MHz observed near the $z$ axis in horse HbNO.[11] The [$^{14}N$]histidine splitting was not resolved in horse HbNO[11] crystals but has been observed in other nitrosylhemes.[28] The hyperfine interaction is best resolved near the $z$ axes of the $g$ anisotropy.

We tentatively assign the a subunit to $\alpha$ and the b subunit to the $\beta$ subunit as follows. The Fe–N bond directions from the horse

(27) Schonland, D. S. *Proc. R. Soc. London* **1959**, *73*, 788.
(28) (a) Dickinson, L. C.; Chien, J. C. W., *Biochem. Biophys. Res. Commun.* **1974**, *59*, 1272; (b) *J. Am. Chem. Soc.* **1971**, *93*, 5036.

HbNO crystal structure[7] agree with the heme normals from the EPR of horse met-hemoglobin.[29] Both the $\beta$ heme normals and Fe–N directions lie in the horse *ab* plane or in a plane 8° from the *a* axis. On the other hand, the horse $\alpha$ heme normals[29] and Fe–N directions[7] lie in a plane rotated between 13° and 20° from the *a* axis about *b*. Perutz[30] predicts a relation between the molecular orientation in horse and human hemoglobin crystals on the basis of crystal optical properties and an assumption that the heme dyad axes correspond. The molecular direction of the horse hemoglobin *a* crystal axis corresponds to a molecular direction either 15 or 35° from the tetragonal *c* axis in human hemoglobin crystals.[30] Molecular packing considerations make the 15° figure most likely.[31] The *z* axes of the *g* factor anistropy of the HbNO subunit will be close to the Fe–N and heme normal directions.[2-4] The preliminary analysis of the experimental *g* factor anistropy puts the *z* axes of the b subunit in a plane about 13° from the *c* crystal axis while the *z* axes of the a subunit lie in a plane at least 35° from the *c* axis. Perutz'[30] relation therefore leads us to associate the $\alpha$ subunit in horse hemoglobin with the a subunit and the $\beta$ with the b subunit.[32] While this association is quite clear, the assignment is nonetheless indirect, and we refrain from using the $\alpha$ and $\beta$ designation for the results at this time.

An apparent contradiction with this assignment should be clarified. There is evidence that $\beta$-NO heme subunits randomly oriented in frozen solution have more poorly resolved EPR spectra than $\alpha$-NO subunits.[3,9] Along the *c* axis in our single crystals, the imidazole-$^{14}$N hyperfine intraction in the b subunit is resolved while it is not in the a subunit. However, well-resolved imidazole-$^{14}$N hyperfine interaction is also observed in the a subunit around 35° from the *c* axis. Therefore, the observations are simply explained by the different orientations of the heme subunits in the crystal without invoking any inherent differences in the subunits which may bear on the assignment.

**(II) NO Uptake.** Horse HbNO crystals have been grown from HbNO solutions prepared by reacting NO with methemoglobin, a reaction essentially complete in 5 min at room temperature.[11] The human HbNO crystal growth, expected to be more difficult, was first attempted by conversion of $HbO_2$ with NO gas because horse HbNO crystals had been prepared successfully from methemoglobin crystals with NO gas over several days time.[7] However, since our best attempts to purify NO gas and to eliminate $O_2$ failed to prevent protein denaturation, we presently generate NO in situ with nitrite[25,26] and ascorbate.

The HbNO spectrum resulting from the exchange of $O_2$ for NO in the $HbO_2$ crystals in this way is described in I. The number of HbNO EPR lines and the symmetry relations between them are displayed in Figure 2. They are in one-to-one correspondence with the $HbO_2$ space group symmetry, the numbers of molecules per unit cell, and the molecular subunit arrangement. This accords with the expected $HbO_2$ and HbNO structural similarity.[7] The $\alpha$ and $\beta$ subunits have significantly different *g* values as given in Table I but the differences are probably too small to be pH or phosphate induced.[9,18] The strict one-to-one correspondence demonstrates that only a local structural change accompanies $O_2$–NO exchange in the presence of bound NO, insignificantly altering the spectrum of any neighbor NO–heme subunit.

At the outset of this work we noted a puzzling crystal-to-crystal variation in the relative intensity of the two low-field features in the H$\|$*c* spectrum at ~85 K indicated in Figure 4. The spectrum simulation shows them to be near the extreme low-field hyperfine lines of the $\alpha$ and $\beta$ spectra. The ratio appears to vary monotonically with the length of time of the nitrite–ascorbate treatment as shown in the series of spectra in Figure 4. The low-field feature

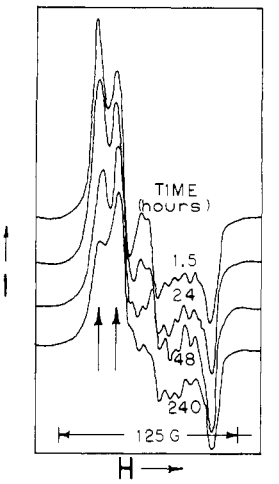


**Figure 4.** The EPR spectra of four HbNO-containing crystals at ~85 K with $H\|c$ after treatment with ascorbate–nitrate for the indicated times. The centers of the 250-G sweeps are 3245 G, and the microwave frequencies are 9.20 GHz.

is an a-subunit line, and it predominates early in the treatment. This presumably indicates that exchange on the b subunits is relatively slower than on the a subunits. That some difference exists in the subunit rates is not surprising in view of Gibson's demonstration that ligand-binding rates are different in general for $\alpha$ and $\beta$ chains.[15b-f]

The number ratio of nitrosylated a and b subunits in the crystal are estimated from the measured spectra. In the $H\|c$ spectrum simulation in Figure 3, the maximum in the derivative of the low-field hyperfine line lies downfield from any significant b-subunit intensity. Likewise, the b-subunit high-field minimum lies above any a intensity. Each experimental subunit intensity is normalized to the corresponding feature in the simulated subunit spectrum. The normalized intensity ratio is the estimate of the ratio of the numbers of a and b subunits in the crystal.

The change in a:b ratio with time gives a glimse at the nature of nitrosylation. In the spectra in Figure 4, the ratios are 2.5 at 1.5 h, 2.1 at 24 h, 1.4 at 48 h and at 240 h. The leveling off at a value of 1.4 at 48 h probably represents full nitrosylation (a:b = 1). The discrepancy of 40% is within the uncertainties in the line-width simulation of the hyperfine interaction used in normalization. While half-nitrosylation of each kind of subunit would also be consistent, this is unlikely in view of the very large $O_2$–NO exchange partition constant $2.4 \times 10^5$ in solution.[24] The first datum indicates that the a subunits exchange their $O_2$ for NO at least 2.0–2.5 times faster than b subunits in the first 1.5 h of treatment. At this time approximately two a subunits are nitrosylated for every one b subunit. After this time a much slower growth of the relative number of b subunits occurs until the ratio approaches 1 after about 48 h when the crystal is presumably fully nitroslyated. The more rapid replacement rate observed for the a subunit seems to be in qualitative agreement with previous solution measurements of $\alpha$-chain replacement rates greater than that of the $\beta$ chains.[33] Further EPR studies are in progress to measure absolute NO uptake at more frequent intervals and with various nitrite–ascorbate concentrations.

**(III) Temperature and Power Dependence.** The NO uptake experiments (II) indicate that the HbNO EPR spectra belong to crystals whose molecules have a least three nitrosylated subunits. In methemoglobin crystals the intra- and intermolecular magnetic dipole interactions between nearest heme subunits are typically several megahertz times *h*.[34] Since the heme–heme distances and the magnetic moment in HbNO are comparable, heme–heme dipolar contributions may also be appreciable in the NbNO line width.

(29) Bennet, J. E.; Gibson, J. F.; Ingram, D. J. E. *Proc. R. Soc. London, Ser. A* **1957**, *A240*, 67.
(30) Perutz, M. F. *Acta Crystallogr.* **1953**, *6*, 859.
(31) Bragg, L.; Howells, E. R.; Perutz, M. F. *Proc. R. Soc. London, Ser. A* **1953**, *A222*, 33.
(32) The other association consistent with Perutz'[30] 15° horse–human angle puts the *z* axis pair planes of both $\alpha$ and $\beta$ subunits within 10° of the tetragonal axis contrary to experiment. Moreover, this association puts the pleochroic axis in horse hemoglobin more than 14° from the heme normal vector average rather than within 4° in the acceptable association.
(33) McDonald, M. J.; Noble, R. W. *J. Biol. Chem.* **1972**, *247*, 4282.
(34) Brill, A. S. Hampton, D. A. *Biophys. J.* 1979 *25*, 313.

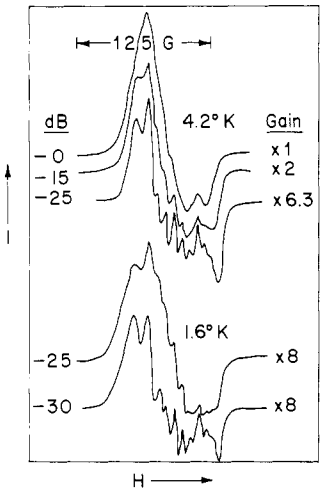


**Figure 5.** Examples of the temperature and power dependence of the HbNO single-crystal EPR spectrum at liquid-helium temperatures with $H\|c$. The fields at the center of the 125 G-measure shown were 3160 G. The full scans were 250 G, and the frequencies were 9.00 GHz.

Heterogeneous dipolar broadening may be evident in the EPR spectrum at 80–90 K. The $H\|c$ spectra are somewhat better simulated with Gaussian hyperfine lines than with Lorentzians. The large line-width anisotropy observable, for example, along the *a*, *b*, and *c* axes in Figures 1 and 2, is consistent with dipolar broadening. The magnitude of the line-width anistropy is too great, however, for heme–heme dipolar contributions only. For example, some of the line width when $H\|a$ and $H\|b$ clearly must come from unresolved $^{14}NO$ and [$^{14}N$]histidine hyperfine.

Representative spectra with $H\|c$ from a study of the power dependence at 4.2 K and below are shown in Figure 5. The hyperfine lines of the b subunit at 4.2 K are clearly sharper by at least half their width than at 80–85 K. The temperature-dependent broadening is presumably homogeneous and may occur via heme–heme magnetic dipolar interactions with flipping spins on neighbor subunits.

The saturation behavior provides additional information about the relaxation times associated with the homogeneous broadening. At 80 K with $H\|c$, neither the $\alpha$ nor $\beta$ subunits can be saturated appreciably with the $\sim$1.5 W power employed. Figure 5 demonstrates that the b subunit is apparently more easily saturated at 4.2 K than the $\alpha$ subunit. The power reduces the b-subunit hyperfine line intensity by about half at 20 dB. We estimate 5 MHz as the maximum possible residual homogeneous line width at 4.2 K, and it corresponds to a lower $T_2$ limit, $T_2 \geq 3.1 \times 10^{-8}$ s. Unsuccessful efforts to observe electron-spin echoes in highly nitrosylated crystals under these conditions with an instrument described elsewhere[35] constitutes an upper limit to $T_2 \leq 10^{-6}$ s. The microwave magnetic field $H\mu = 1.2$ G in the rotating frame at full power has also been determined in other spin–echo experiments.[35] This field value and the condition for half-saturation of the b subunit give the bound for $T_1$ corresponding to the $T_2$ limits above, $2.2 \times 10^{-7}$ s $\leq T_1 \leq 7.2 \times 10^{-6}$ s. These bounds imply near equality of $T_1$ and $T_2$, and this is consistent with spin–lattice and spin–spin relaxation occuring via the same mechanism.

The power dependence of the spectra in Figure 5 merits further comment. If the bath of equivalent b-subunit spins were being saturated fully and completely independently, the spectrum of the equivalent a subunits would remain behind unaltered except for a degree of saturation. However, the partially saturated spectrum actually left behind, for example, at 4.2 K and 0 dB, is clearly not the three-line hyperfine pattern of the a subunit. The cooperative saturation of $\alpha$ and $\beta$ subunits results from cross relaxation between subunits occurring at a rate comparable with spin–lattice relaxation at 4.2 K. This effect is also consistent with relaxation via heme–heme dipolar coupling. Presumably interactions between like subunits are also important because their interheme distances are comparable.[34]

(35) Doetschman, D. C.; Fierstein, E. S.; Michaelis, J.; DeSantolo, A. M.; Utterback, S. G. *Chem. Phys. Lett.* **1980**, *74*, 539.

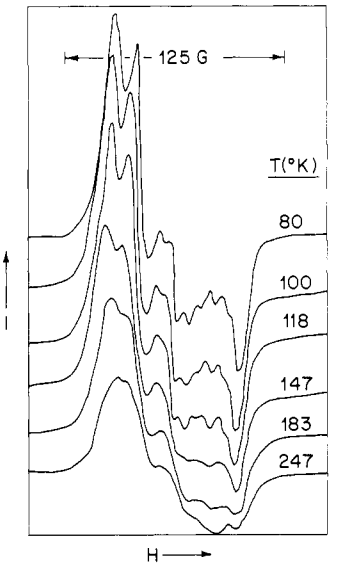


**Figure 6.** Temperature dependence of HbNO crystal EPR spectrum with $H\|c$. The field at the center of the 250-G sweeps is 3240 G, and the microwave frequencies are 9.195 GHz.

In Figure 6 is shown the temperature dependence of the $H\|c$ spectrum between 80 K and room temperature at full microwave power, with which there is negligible saturation. The loss of the a- and b-subunit hyperfine features and the evolution of the general shape of the spectrum as temperature is elevated are qualitatively similar to the spectrum change with increasing power at low temperatures in Figure 5. In neither case does the spectrum appear to be comprised simply of its broadened components.

It should be emphasized that the effects discussed here cannot be attributed to the saturation broadening of narrow components of the lines. As mentioned previously, the effective microwave magnetic field at 0 dB is about 1 G. The line-width changes shown in Figures 5 and 6 are obviously about 10 times greater even at many 0.1 of decibels down in power.

The simularity can be explained qualitatively as follows. At 4.2 K, microwave pumping and $\alpha$–$\beta$ cross relaxation are fast compared with spin–lattice relaxation. At 247 K, the roles of the lattice and microwave source are resversed so that spin–lattice relaxation and cross relaxation are fast compared with microwave pumping. Cross relaxation at 247 K driven predominantly by contact with the lattice gives a kind of averaged spectrum of the subunits. A similar spectrum is found at 4.2 K when cross relaxation is driven by the microwaves. Apparently at 80–85 K spin–lattice relaxation has increased leaving the cross relaxation and microwave pumping rates relatively slow. Therefore negligible saturation or cross relaxation appears at 80–85 K.

Variation of the field direction changes the relative orientation of heme–heme directions and the overlap of lines in the spectrum. Additional studies of this kind at field orientations besides $H\|c$ will illuminate further the role of heme–heme magnetic dipolar interactions in these processes. Hyperfine structure is also rarely resolved along other magnetic field directions than the *z* axes of *g* and may signal some kind of motion of the NO group around this axis that deserves further study.

**(IV) HbNO Photodissociation and Thermal Recombination.** The exchange of NO for $O_2$ in $HbO_2$ crystals was well-behaved, conformed to the crystal space group and was examined satisfactorily by means of single-crystal HbNO EPR. This suggested that HbNO photodissociation and recombination could be monitored continuously by means of the EPR spectrum of an HbNO crystal oriented in the EPR cavity at low temperatures. Several Hg-Xe lamp irradiations of crystals at $\sim$95 K gave no perceptible change in the HbNO spectrum. Moreover no transients were observed on an oscilloscope display of the HbNO signal at a millisecond time response with pulsed $N_2$ laser irradiation. These

uneventful experiments led to the sucessful photolysis at liquid-helium temperatures described presently.

An NbNO crystal is oriented with $H \| c$ at 80 K and cooled with liquid helium pumped to 1.7 K. The crystal alignment is checked and the spectrum is recorded before photolysis. The crystal is irradiated until the HbNO EPR spectrum drops to less than 6% of its original intensity within ~2 min. No HbNO recombination nor any other spectrum is observed at 1.7 K after irradiation. The residual few percent of HbNO have a number ratio of a:b subunits that is as little as $^2/_3$ in an originally fully nitrosylated crystal. A unimolecular HbNO recombination with a rate constant above $\sim 10^{-4}$ s$^{-1}$ would be detected in the experiment after irradiation. The subunit photodissociation quantum yields per photon of light absorbed in the Q band are estimated greater that $10^{-3}$. They appear to differ very slightly in the $\alpha$ and $\beta$ subunits.

After the liquid helium vaporizes, the spectrum is scanned repetitively as the sample warms up to 85 K. There is little if any (≤5%) recombination below 70 K in about 20–30 min. Above 70 K the rate becomes observable and recombination is at least 80% complete by 85 K within 10–20 min at most. The temperature stabilizes at 85 K, and the spectrum changes no further. The $\alpha$:$\beta$ number ratio returns to within 1% of its value before photolysis, and the spectra are almost indistinguishable.

The experiment demonstrates rapid HbNO photolysis at 1.7 K where recombination rates are comparatively small. The recombination becomes appreciable above ~70 K and increases rapidly with temperature to swamp, apparently, the incompetitive photolysis at 95 K. The minimum activation energy estimated from the experiment is about 7 kJ mol$^{-1}$ (600 cm$^{-1}$). Energy barriers of 10 kJ mol$^{-1}$ and 4 kJ mol$^{-1}$ were found for recombination of carbonmonoxymyoglobin[21,22] and -$\beta$-Hb chains,[19] respectively. However, in our HbNO recombination there is apparently no fast low-temperature tunnelling.[19] Measurements of the quantum-yield wavelength dependence and recombination rate determinations at fixed temperatures should be made to understand better the photolysis and recombination mechanisms.

## Conclusions

The EPR spectrum of HbNO made from $HbO_2$ crystals conforms to the $HbO_2$ crystal symmetry. The principal $g$ values and axes of the $\alpha$ and $\beta$ subunits were measured. The spectrum with the field along the tetragonal crystal axis was simulated by a sum of two subunit spectra. One subunit displays both $^{14}$NO and [$^{14}N$]histidine hyperfine splittings while the other displays only the $^{14}$NO pattern. Association of the $z$ principal $g$ axis with the heme normal is consistent with the hemoglobin crystal structures and makes possible a tentative assignment to the $\alpha$ and $\beta$ subunits.

The uptake of NO from solution by the $\alpha$ and $\beta$ subunits in $HbO_2$ is crystallographically well-behaved according to EPR studies. It is accompanied by no detectable EPR changes in subunits already bound to NO, and the small differences in the $\alpha$ and $\beta$ $g$ values suggest no pH- or phosphate-induced effects. The a subunits exchange at least twice as fast as b subunits in the first 1.5 h of treatment yielding about two a subunits for every one b subunit. The last b subunit appears to exchange very slowly, and full nitrosylation is reached after about 48 h.

The temperature and power dependence of the HbNO EPR spectrum has the earmarks of magnetic dipolar interaction between the subunit spins. Transfer of saturation between unlike subunits appears directly in the spectrum. At 4.2 K, $T_1$ and $T_2$ are comparable, so that transverse relaxation may also be via heme–heme dipolar interactions. Some of the line-width anisotropy observed must arise from unresolved hyperfine interaction.

Rapid photolysis of HbNO occurs with a quantum yield greater than $10^{-3}$ at 1.7 K, a temperature at which recombination is not occurring with a unimolecular rate over $10^{-4}$ s$^{-1}$. As the temperature is raised, no appreciable recombination occurs below 70 K, but it becomes competitive with photolysis above 85 K. A minimum activation energy of 7 kJ mol$^{-1}$ is estimated for recombination.

**Acknowledgment** is made to the donors of the Petroleum Research Fund, administered by the American Chemical Society, to the SUNY Research Foundation Joint Awards Council and University Awards Committee. The project is supported in part by NIH Grant No. S07RR07149-05 and -06 awarded by the BRSG Program, Division of Research Resources. We are grateful for the scientific help and advise of Professor Anna Tan-Wilson and for the cooperation of our cryogenics engineer, Mr. Weldon Willard, and the Broome County Red Cross Blood Bank.

# Simple Molecular Orbital Explanation for "Bay-Region" Carcinogenic Reactivity

**John P. Lowe* and B. D. Silverman‡**

*Contribution from the Department of Chemistry, The Pennsylvania State University, University Park, Pennsylvania 16802, and the IBM Thomas J. Watson Research Center, Yorktown Heights, New York 10598.* *Received October 27, 1980*

**Abstract:** Polycyclic aromatic hydrocarbons containing a "bay region" form triol carbonium ions with special ease. This is shown to be due to the fact that such ions can have the $-CH^+-$ group of the triol ring attached to a carbon atom which is a nearest neighbor to a ring fusion site.

## Introduction

Identification[1-3] of the enhanced carcinogenicity of the 7,8-diol 9,10-epoxide of benzo[*a*]pyrene has focused attention on vicinal diol epoxides as likely candidates for the ultimate carcinogens of polycyclic aromatic hydrocarbons (PAH). Investigation of the relative carcinogenic activity of different PAH has led to the recognition that diol epoxides on angular benzo rings in which the epoxide ring forms part of a "bay region" are the most reactive of all possible isomeric diol epoxides of a given PAH.[4] The

* Address correspondence to this author at The Pennsylvania State University.

‡ IBM Thomas J. Watson Research Center.

(1) Borgen, A.; Darvey, H.; Castagnoli, N.; Crocker, T. T.; Rasmussen, R. E.; Yang, I. Y. *J. Med. Chem.* **1973**, *16*, 502–506.

(2) Sims, P.; Grover, P. L.; Swaisland, A.; Pal, K.; Hewer, A. *Nature (London)* **1974**, *252*, 326–328.

(3) Jerina, D. M.; Lehr, R.; Schaeffer-Ridder, M.; Yagi, H.; Karle, J. M.; Thakker, D. R.; Wood, A. W.; Lu, A. Y. H.; Ryan, D.; West, S.; Levin, W.; Conney, A. H. *Cold Spring Harbor Conf. Cell Proliferation* **1977**, *4*, 639–658.

0002-7863/81/1503-2852$01.25/0 